The Anti-Angiogenesis Mechanism of Geniposide on Rheumatoid Arthrits is Related to the Regulation of PTEN

Yanhong Bu (1339645973@qq.com)
Anhui University of Traditional Chinese Medicine https://orcid.org/0000-0002-3261-9276
Hong Wu
Anhui University of Traditional Chinese Medicine https://orcid.org/0000-0002-5427-6200
Ran Deng
Anhui University of Traditional Chinese Medicine
Yan Wang
Anhui University of Traditional Chinese Medicine

Research Article

Keywords: PTEN, Geniposide, angiogenesis, rheumatoid arthritis, human umbilical vein endothelial cells, phosphatidylinositol 3-kinase

Posted Date: January 18th, 2022

DOI: https://doi.org/10.21203/rs.3.rs-1240306/v1

Abstract

Rheumatoid arthritis (RA) is a systemic immune disease characterized by joint inflammation and pannus. The nascent pannus contributes to synovial hyperplasia, cartilage and tissue damage in RA. Based on the previous study on the anti-inflammatory effect of Geniposide (GE) on arthritis rats, this study aims to explore the therapeutic effect and potential mechanism of GE on RA angiogenesis, involving the participation of phosphate and tension homology deleted on chromosome ten (PTEN) and downstream pathways. Clinical manifestations, synovial pathomorphology, microvessel density and the level of angiogenesis-related factors were used to evaluate the therapeutic effect of GE on adjuvant-induced arthritis (AA) rats. The proliferation, migration, tube formation of human umbilical vein endothelial cells (HUVECs) indicate the degree of angiogenesis *in vitro*. Lentivirus overexpression of PTEN was employed to elucidate the potential mechanism. The results showed that GE improved the degree of arthritis and angiogenesis in AA rats. PTEN was decreased significantly *in vivo* and *in vitro*, and over-expression of PTEN improved the biological function of HUVECs to inhibit angiogenesis. GE inhibited the proliferation, migration and tubule formation of HUVECs and plays an anti-angiogenesis role *in vitro*. Mechanism study showed that PTEN expression was increased and p-PI3K and p-Akt expression was decreased with GE treatment. It suggests that GE up-regulated the expression of PTEN and inhibited the activation of PI3K-Akt signal, which plays a role in inhibiting angiogenesis in RA *in vivo* and *in vitro*.

1. Introduction

Rheumatoid arthritis (RA), as a chronic and inflammatory autoimmune disease, is characterized by multiple inflammatory cells infiltration, pannus formation and synovial hyperplasia. Among them, angiogenesis runs through the whole process of RA, which is one of the main reasons of RA with long-standing incurability [1, 2]. Neovascularization provides oxygen, nutrients and signal molecules for highly proliferative synovial tissue, maintains the continuous proliferation of fibroblast-like synoviocytes (FLS), and increases the recruitment of inflammatory cells into the tissue, leading to synovitis and tumor-like proliferation of FLS. The abnormally proliferating FLS aggravates the process of angiogenesis by secreting inflammatory cytokines and/or angiogenic factors, such as growth factors, hypoxia inducible factors, chemokines, matrix metalloproteinases and adhesion molecules [3, 4].

Angiogenesis is the process of forming new blood vessels from the pre-existing vessels, which has been proved to be one of the pathogenesis of RA [5]. Under physiological conditions, blood vessels remain quiescent and rarely form new branches. Whereas in developmental, tissue repair or pathological situations, endothelial cells (ECs) form new blood vessels through a series of complex processes. Firstly, extracellular matrix is degraded under the stimulation of angiogenesis signals, such as vascular endothelial growth factor (VEGF), which is produced by changes in the external environment or surrounding tissues. Activated ECs rapidly proliferate and migrate into tissues to form new lumens [6,7]. Therefore, the inhibition of angiogenesis caused by the proliferation and migration of ECs in RA has become an important goal in the treatment of RA.

In addition to angiogenic factors or extracellular signals, the genetic changes and mutations of tumor suppressor genes also trigger the process of angiogenesis. Phosphate and tension homology deleted on chromosome ten (PTEN) was first known as a tumor suppressor gene, which is involved in various cellular processes including cell proliferation, survival, angiogenesis, and tumor growth by regulating intracellular signaling [8–10]. PTEN, as a negative regulator of PI3K, regulates PI3K-Akt signal and participates in angiogenesis. The direct evidence is that the extensive sprouting of new blood vessels and the enlargement of original blood vessels can be observed by the over-expression of PI3K and Akt by RCAs retroviral vector [11]. In addition to inhibiting PI3K activation, some studies have found that PTEN regulates the expression of VEGF by activating JNK and ERK signals and participates in the process of angiogenesis [9, 12,13]. This provides evidence for the important role of PTEN in regulating cell growth, migration and angiogenesis.

Geniposide (GE) is a kind of iridoid glycoside obtained from *Gardenia jasminoides* Ellis by modern technology of traditional Chinese medicine, which has pharmacological effects of anti-inflammatory and anti-angiogenesis [14]. Previous work of our group focused on the therapeutic effect of GE on experimental arthritis. It was found that GE regulates the VEGF level in FLS and restores the dynamic balance of pro/ anti-angiogenic factors in AA rats [15,16]. The purpose of this study is to explore the role of PTEN in angiogenesis of AA rats and the relationship between downstream PI3K-Akt signal and the anti-angiogenesis of GE *in vivo* and *in vitro*.

2. Materials And Methods

2.1 Drugs and reagents

Geniposide is a white powder with 98% purity and purchased from Guangxi Shanyun Biochemical Technology (Guangxi, China). Frennd's complete adjuvant (FCA) was obtained from Sigma (St. Louis, MO, United States). Tripterygium Glycosides (TG) was obtained from Huitian Biopharmaceutical (Fujian, China). PTEN inhibitor Bpv (HOpic) and PI3K inhibitor LY294002 were obtained from Selleck Chemicals (Texas, United States). Fetal bovine serum (FBS) and Dulbecco's modified Eagle's medium (DMEM) were purchased from Thermo Scientific (Hudson, NH, United States). PTEN over-expression lentiviral vector was obtained from Hanbio Biotechnology (Shanghai, China). kFluor488 Click-iT Edu imaging detection kit was obtained from KeyGEN BioTECH (Nanjing, China). Rabbit anti-PTEN antibody (ab170941) was purchased from Abcam (Cambridge, United Kingdom). Rabbit anti-PI3K antibody (#4257), anti-AKT antibody (#4691), anti-p-PI3K antibody (#17366) and anti-p-AKT antibody (#4060) were purchased from Cell Signaling Technology (Boston, United States). Monoclonal antibodies against CD31 (66065-2-lg), β-actin (66009-1-lg) were obtained from Sanying Biotechnology (Wuhan, China).

2.2 Animals and cells

Healthy Sprague-Dawley (SD) rats treated with complete Freund’s adjuvant (FCA) at 0.1mL by subcutaneous administration of the left posterior paw to induce adjuvant arthritis, an animal

experimental model of RA. Rats without paw swelling were given 0.05 mL FCA supplement before the 7th day. The model was evaluated after 17 days, including arthritis index, paw swelling, and mobility score, oral administration was continued for a week. Normal control and model group were given the same dose of normal saline. The specific experimental design is shown in Fig. 1. Male SD rats of Specific pathogen Free (SPF) grade were used in this experiment and weighed 160-190 g. The quality testing unit is Shandong Animal Experimental Center, and the ethics report is issued by the experimental animal ethics committee of Anhui University of traditional Chinese medicine. Human umbilical vein endothelial cells (HUVECs) were provided by BeNa Culture Collection (BNCC, Beijing, China) (No 347734)and grown in an epithelioid adherent manner.

2.3 Evaluation of AA rat model

Arthritis index, paw swelling, mobility score were used to evaluate the model. The arthritis index was judged according to the degree of joint swelling, and the specific criteria were as follows: 0 point indicating normal without swelling; 1 point indicating slight swelling and erythema of ankle joint; 2 points indicating slight swelling and erythema from ankle joint to toe joint or metacarpal joint; 3 points indicating moderate swelling and erythema from ankle joint to toe joint or metacarpal joint; 4 points indicating severe swelling and erythema from ankle joint to toe joint. The maximum score of each rat was 12. Paw swelling was measured with a foot volume meter every 3 d after the appearance of inflammation, and the degree of foot swelling was calculated (Δ mL=foot volume after modeling-foot volume before modeling). Mobility score was performed every 3 d by the non-participants personnel. Each rat was placed in a box with a certain movement space and observed for more than 30 s. The specific scoring criteria are as follows: 0 point for only lying down; 1 point for crawling; 2 points for standing but difficulty walking; 3 points for walking but difficulty running; 4 points for normal walking.

2.4 Histopathological assessment

The synovial tissue was fixed in 4% paraformaldehyde tissue solution, dehydrated and embedded in paraffin. The sections were then stained with Hematoxylin and Eosin (H&E). The pathological characteristics of synovial tissue were observed under microscope (OLYMPUS BX51, Germany).

2.5 Immunohistochemistry

The expression level of CD31 on the surface of vascular endothelial cells (VEC) in synovial tissue, a specific marker of VEC, was detected by specific anti-CD31 antibody. Synovial tissue was first fixed with formalin and then embedded in paraffin. Sections were incubated with H_2O_2 to block endogenous peroxidase. Then, goat anti-CD31 (1:100) and VEGF antibody (1:150) were incubated overnight at 4 ^{o}C. Finally, sections were incubated with secondary antibodies, treated with 3, 3 '- diaminobenzidine and counterstained with hematoxylin. VEC positive for CD31 clustered into brown as a single microvessel. The average optical density of positive staining was quantified as the relative expression level of the target protein by Image J software analysis.

2.6 ELISA

The level of angiogenic factor in serum of AA rats was measured by VEGF specific ELISA kit according to the manufacturer's protocol (J&L Biological, China). Absorbance was determined at 450 nm to quantify the samples. Six replicates were set for each sample.

2.7 Cell culture

HUVECs were cultured in high-glucose Dulbecco's modified Eagle's medium containing 10% fetal bovine serum and 1% penicillin-streptomycin solution (100×). In order to induce inflammatory conditions, HUVECs stimulated by TNF-α was selected to establish an inflammatory model *in vitro*. In addition, according to the previous protocol, the cell co-culture technology *in vitro* has also been applied to better simulate the inflammation *in vivo* and compare with TNF-α stimulation alone. The specific method was that FLS derived from synovial tissue of AA rats by *in vitro* culture were treated with TNF-α (10 ng/mL) for 24 hours. The conditioned medium (FLS-CM) was collected and diluted to different concentrations with DMEM (0%, 5%, 25%, 50%, 75% and 95%) to stimulate HUVECs for 24 hours.The optimal stimulation concentration was selected for experiments.

2.8 Infection and validation of lentivirus

PTEN over-expression lentiviral vectors were obtained from Hanbio Biotechnology (Shanghai, China). Lentivirus infection of HUVECs induced over-expression of PTEN, and an empty GFP vector (Lv-GFP) was used as a control. After infection, the results of over-expression were detected by Immunofluorescence and RT-qPCR.

2.9 Immunofluorescence staining

HUVECs were seeded on the round coverslip at a density of 10^5 cells/mL. After 4% paraformaldehyde fixation, 0.5% TritonX-100 permeabilization, and BSA blocking, staining with rabbit anti-CD31 primary antibody was performed overnight. Goat anti-rabbit lgG (H+L) conjugated Cy3 (550076, ZEN-BIO Science) was used as a secondary antibody. The nuclei were stained with 4, 6-diamidino-2- phenylindole (DAPI) and the slides were made after dropping anti-quenching reagent (PD131-25, Beyotime). Finally, the slides were photographed and analyzed under a fluorescence microscope (OLYMPUS BX51, Germany). .

2.10 Edu proliferation assay

HUVECs were seeded on the round coverslip in 48-well plates at a density of 10^5 cells/mL. Different concentrations of GE or inhibitors Bpv were administered after incubation in the DMEM medium containing 10% FBS for 24 hours. The following protocols were performed by kfluor488 Edu cell proliferation detection kit (KeyGEN BioTECH, Nanjing, China). After successful staining, the coverslip were then coated with nail polish on the slide. Finally, it was imaged and analyzed under fluorescence microscope.

2.11 Cell cycle analysis

HUVECs were treated with different concentrations of GE or Bpv to analyze the cell cycle when growing to a density of 50%. The cells were digested and fixed in 70% ethanol overnight at 4 ^{o}C. The cells were resuspended in PBS the next day, and stained with 400 μL propidium iodide (PI) solution (50 μg/mL) (Solarbio, P8080, Beijing, China) and 100 μL RNase A (100 μg/mL) (Solarbio, R1030, Beijing, China) for 30 min in the dark. Finally, it was analyzed by flow cytometry (Beckman Coulter, FC500) and FlowJo software (Version 10.6.0).

2.12 Cell counting kit-8 assay

The cells were planted in 96-well plates at the density of 10^4 cells/well and cultured in 37 ^{o}C incubator for 24 hours. Six wells in each group were treated with TNF-α (10 ng/mL) or GE (25, 50, 100 μM) and incubated for 24 hours. Then 10 μL of CCK-8 solution was added to each well and continue to culture for 2 hours. The optical density (OD) at 450 nm was measured with a microplate reader (SpectraMax iD3, Molecular Devices, the United States), and the cell proliferation rate was calculated based on OD450 values.

2.13 Wound-healing analysis

The wound-healing experiment was used to determine the migration ability of cells. HUVECs were seeded into 6-well plates at a density of 6×10^5 cells/well, and cells were cultured to adherent and grown to a density of 90%. The cells were scratched vertically with 200 μL sterile pipette and ruler, leaving a vertical line. The slipped cells were washed, and photographed under a microscope observation. This time point was set at 0 h. Next, TNF-α (10 ng/mL) or GE (25, 50, 100 μM) were treated and photographed after incubation for 6, 12, 24 hours, respectively. The scratch area at different time points was measured by Image J software, and the rate of wound healing was calculated to represent the migration ability of cells.

2.14 Vertical migration analysis

HUVECs (10^5 cells/mL) were seeded in the upper chamber of a polycarbonate transwell chamber (Corning, United States) with 8 μm pore membranes in order to evaluate the vertical migration ability of cells. The upper chamber medium was replaced with the low concentration FBS (5%) medium containing TNF-α (10 ng/mL) or GE (25, 50, 100 μM), and the lower chamber was the medium containing 10% FBS. After 24 h of culture, the chamber was removed and washed with PBS once. The cells that did not pass through the membrane were carefully wiped off with a cotton swab, and the cells under the membrane were fixed with 4% paraformaldehyde. The membrane was dried naturally and then stained with crystal violet for 20 min. Finally, the membrane was fixed on a glass slide and observed under an inverted microscope (Leica DMI6000B, Germany). The number of migrating cells was analyzed by Image J software.

2.15 Tube formation assay

Before the experiment, the 96-well plate and sterile pipettes were pre-cooled at -20 ^{o}C in advance, whereas Matrigel (Corning, United States) was thawed at 4 ^{o}C. 50 μL of Matrigel was taken in a 96-well plate and incubated for 30 min to solidify in a 37 ^{o}C incubator. Cell suspensions made of different groups were seeded into 96-well plate containing Matrigel at a density of 2×10^{4} cells/mL. Images were taken by a microscope after 24 hours of incubation (Leica DMI6000B, Germany). The number of tubes and the length of branches were calculated by Image J software to represent the lumen forming ability of cells.

2.16 Western blot analysis

HUVECs of different groups grown to 80% were washed three times with ice-cold phosphate buffered saline (PBS). 500 μL RIPA lysate containing 1% PMSF protease inhibitor was lysed and then centrifuged at 12000 rpm at 4 ^{o}C for 30 min. The supernatant was collected and the total protein was quantified by BCA protein quantification kit (Beyotime, China). The equivalent protein samples were separated by 8-10% sodium dodecyl sulfate-polyacrylamide gel electrophoresis and transferred to PVDF membranes (Biosharp,Shanghai, China) under constant current condition of 200 mA. The membrane was blocked in 5% (w/v) skimmed milk for 2 h to block non-specific protein binding. The membrane was incubated with primary antibody at 4 ^{o}C overnight after washing with Tris-buffered saline containing Tween-20 (TBST). After that, it was incubated with goat anti-rabbit or mouse IgG horseradish peroxidase conjugated secondary antibody for 1 h at room temperature. The levels of each protein were normalized to β-actin. The protein bands were exposed with the alpha view SA system (protein simple, California, United States) and analyzed by image software.

2.17 Quantitative real-time polymerase chain reaction (RT-qPCR) assay

Total RNA from different groups of HUVECs was extracted using Trizol reagent (Invitrogen, United States). The concentration of RNA was determined, and samples with purity (A260 / A280) between 1.8-2.1 were selected for the next step. The extracted total RNA was reverse transcribed into cDNA using the EasyScript® All-in-One First-Strand cDNA synthesis kit (Transgen Biotech, China). The expression of the target gene was relatively quantified by SYBR RT-PCR in Lightcycle 480 system (Roche, United States). PCR conditions was 95 ^{o}C for 10 min, 40 cycles of 95 ^{o}C for 20 s, and finally 55 ^{o}C for 30 s. The relative mRNA levels was obtained by the $2^{-\Delta\Delta CT}$ method using GAPDH as an internal reference gene. Primer design and synthesis were supported by Sangong Biotech (Shanghai, China). The primers sequences are as follows. PTEN forward: GTTGATGTTTATTTTTTTTAAGTGG and reverse: TATCAAATCTATTTACAACCCCAAT; PI3K forward: ATCGACCTACACTTGGGGGA and reverse: CAATATCTTCTGGCCGGGCT; AKT forward: TGGAGTGTGTGGACAGTGAAC and reverse: AGGTACAGATGATCCATGCGG.

2.18 Statistical analysis

The experimental data are expressed by mean ± standard deviation (SD) and statistically analyzed by SPSS 23.0 software. The significance of differences between groups was compared by one-way ANOVA.

In all results, $P < 0.05$ or 0.01 was considered statistically significant.

3. Results

3.1 GE improved the symptoms of joint inflammation in AA rats

SD rats were injected with FCA for 7 d to induce an AA model. AA rats showed swelling and joint stiffness on the left hind limb, while arthritic nodules appeared at the ankle (Fig. 2A). From the 7 d to the 17 d after modeling, the arthritis index and paw swelling gradually increased, while mobility score decreased, indicating that the modeling was successful. The arthritis index and paw swelling were significantly decreased and mobility score was increased in AA rats after treatment with GE and TG, indicating that GE effectively alleviated joint inflammation in AA rats (Fig. 2B-D). Synovial pathomorphology showed that the synovium of normal rats was composed of 1 or 2 layers of synovial cells overlaid on the surface of connective and adipose tissue, and there was no angiogenesis and aggregation of inflammatory cells. On the contrary, synovial tissues of AA rats showed 3 to 8 layers of hyperplastic synoviocytes, with a large number of inflammatory cells infiltrated the synovium accompanied by subintimal angiogenesis. After treatment with GE or TG, the synovium was significantly thinner and orderly arranged than that in AA group, and the inflammatory cell infiltration and vascular proliferation were relatively reduced (Fig. 2E). It further illustrated that GE alleviated the joint inflammation of AA rats, including the histopathological changes.

3.2 GE inhibited angiogenesis *in vivo* in AA rats

The resulting MVD by the positive expression ratio of CD31 was used to represent the level of angiogenesis *in vivo*. As shown in Fig. 3A, the number of CD31 positive microvessels in AA group was increased compared with the control group, but decreased significantly after GE and TG treatment. MVD quantification was consistent with the above results (Fig. 3B). In addition, immunohistochemical quantitative results showed that GE significantly inhibited the expression of VEGF in synovial tissue. It was also found that PTEN expression was decreased in AA group and GE up-regulated PTEN expression in synovial tissue (Fig. 3C). The level of classical angiogenic factor VEGF shows the degree of angiogenesis. As shown in Fig. 3D, the serum VEGF level in the AA group was increased significantly compared with the control group, and the VEGF level in the GE group was decreased in varying degrees compared with the AA group, which was consistent with synovial tissue. The changes of VEGF level further revealed the anti-angiogenesis effect of GE in AA rats. These results suggest that GE down-regulated angiogenic factors and play an anti-angiogensis role in AA rats.

3.3 Establishment of inflammatory HUVECs model *in vitro*

In order to confirm the role of PTEN in RA *in vitro*, an inflammation cell model of HUVECs and a co-culture cell model of FLS-HUVECs were also established in addition to an AA rat model. First, the appropriate

concentration of TNF-α (0, 1.25, 2.5, 5, 10 and 20 ng/mL) was screened to induce inflammation in HUVECs inflammatory model. The results showed that the proliferation rate of HUVECs was the highest at the concentration of 10 ng/mL (Fig. 4A). The cell co-culture model simulates the real environment between cells very well. HUVECs stimulated by different concentrations of FLS-CM (0, 5%, 25%, 50%, 75% and 95%) were established to determine the optimal co-culture conditions. The proliferation rate of HUVECs stimulated by different concentrations of FLS-CM is shown in Fig. 4B, 50% FLS-CM promoted the proliferation of HUVECs significantly compared with the control group. Western blot showed that PTEN expression in 50%-95% FLS-CM was decreased compared with the control group (Fig. 4C). The above results support the selection of 50% FLS-CM as the stimulation condition for the co-culture model.

Next, the two models were compared by VEGF secretion levels and PTEN expression. Compared with the control group, the VEGF secretion levels was increased in both two models (Fig. 4D). As shown in Fig. 4E, F, PTEN protein expression and mRNA levels were decreased compared with the control group in TNF-α and FLS-CM model. The P values between TNF-α and FLS-CM groups were greater than 0.05, indicating that there was no significant difference in VEGF secretion and PTEN protein and mRNA expression between the two groups. The above results show that these two *in vitro* models simulated the environment of HUVECs in inflammatory and pro-angiogenic media, and the decrease of PTEN expression was consistent with that in synovium of AA rats. For the consideration of experimental operability, the TNF-α inflammation model was selected for subsequent experiments.

3.4 PTEN over-expression inhibited proliferation, migration, and tube formation of HUVECs

Our study showed that the expression of PTEN was decreased in synovium of AA rats. In order to provide more evidence that PTEN is involved in RA angiogenesis, a PTEN lentiviral vector was used to over-express PTEN in HUVECs to assess the effects of over-expression of PTEN on HUVECs proliferation, migration and tube formation *in vitro*. Immunofluorescence and RT-qPCR analysis showed that the expression levels of PTEN protein and mRNA was significantly up-regulated after lentiviral vector infection, demonstrating successful infection (Fig. 5A, B).

The abnormal proliferation of HUVECs was the initial event of angiogenesis. Cell cycle results showed that the G1 phase decreased and the G2 and S phases increased after TNF-α stimulation; Lv-PTEN $^{+}$ up-regulated the cells number of G1 phase cells and down-regulated the cells number of G2 and S phase. It was proved that HUVECs proliferation was promoted under inflammatory conditions, and PTEN over-expression inhibited proliferation (Fig. 5C). Similarly, Edu staining analysis showed that Lv-PTEN $^{+}$ inhibited the proliferation of HUVECs, which was determined by the reduction of green fluorescence representing proliferating cells (Fig. 5D). The migration of HUVECs as the basic behavior of angiogenesis was also examined by wound-healing and transwell assay. The wound healing rate is directly proportional to the ability of cell migration. As shown in Fig. 5E, F, TNF-α stimulation significantly increased the healing rate and the number of migrated cells, while decreased significantly in the Lv-PTEN $^{+}$ group. As a classic model of angiogenesis *in vitro*, HUVECs tube forming experiment is also analyzed.

As shown in Fig. 5G, HUVECs in the TNF-α group was interconnected to form a complete lumen structure, whereas the lumen structure was damaged, the cell edge shrank, and the number of branches decreased significantly after treatment with Lv-PTEN $^{+}$. In conclusion, the over-expression of PTEN maybe is an important factor for inhibition of HUVECs angiogenesis.

3.5 GE up-regulated PTEN to inhibit angiogenesis of HUVECs *in vitro*

To further understand the therapeutic mechanism of GE and the potential involvement of PTEN, the *in vitro* model was used to explore the therapeutic effect of GE on HUVECs angiogenesis. Based on cell cycle analysis, the number of cells in G1 phase decreased and G2 and S phases increased after PTEN inhibitor Bpv treatment. Different concentrations of GE down-regulated the number of G2 and S phase cells, indicating that GE had an obvious inhibitory effect on the proliferation of HUVECs (Fig. 6A). Edu staining analysis also showed that GE inhibited the proliferation of HUVECs (Fig. 6B). As shown in Fig. 6C, D, Bpv induced the migration of HUVECs by inhibiting PTEN. The healing rate and the number of migrating cells were decreased after GE treatment, indicating that GE inhibited HUVECs migration. In addition, the results of tube forming showed that GE also significantly inhibited the tube formation of HUVECs, which was manifested by the reduction of the number of tube and branching length (Fig. 6E). Our results indicate that the GE treatment attenuated the proliferation, migration and tube formation of HUVECs, which may be related to the up-regulation of PTEN expression.

3.6 GE regulated PTEN-PI3K-Akt signaling in HUVECs

Our study shows that over-expressed PTEN plays an important role in inhibiting angiogenesis. However, the mechanism of PTEN in RA angiogenesis remains to be determined. PTEN is closely related to the PI3K-Akt signaling pathway in the pathophysiological process. Expression levels of

PTEN-PI3K-Akt signal axis proteins, including PTEN, PI3K, p-PI3K, Akt, p-Akt, were determined to evaluate the regulatory effect of GE on the signal axis. As shown in Fig. 7A-E, PTEN protein levels was decreased, while p-PI3K and p-Akt protein levels were increased in TNF-α group compared with the control group. GE up-regulated PTEN protein level compared with TNF-α group, which was opposite to that of PTEN inhibitor Bpv group. In addition, exerted significant inhibitory effects on the expression of the proteins involved in the PI3K-AKT signal axis, as in LY294002 group. WB results showed that GE up-regulated PTEN expression and inhibited the activtion of PI3K-Akt signal.

To further confirm the associations among GE, PTEN, and PI3K-Akt signal axis, mRNA levels in HUVECs from each group were evaluated by RT-qPCR. As shown in Fig. 7F, PTEN mRNA level was significantly decreased in TNF-α group, whereas PI3K and Akt mRNA levels were increased compared with the control group. GE up-regulated PTEN and induced significant suppression of PI3K-Akt signal axis-related mRNAs, which was consistent with the WB results. Our results suggested that GE inhibited the activation of PI3K-Akt signal axis by indirectly up-regulating PTEN.

4. Discussion

RA is a chronic disease characterized by persistent inflammation, and the main pathological manifestations are synovial inflammatory hyperplasia, pannus formation, and joint destruction. Angiogenesis, as the basic event of pannus formation, has attracted extensive attention whether contributing to synoviocytes tumor-like proliferation, inflammatory cell infiltration, or articular cartilage destruction [17,18]. The nutrients, oxygen and a variety of signal factors produced by the neovasculature fuel the hypoxia and closed synovial microenvironment undoubtedly, which activates the interaction and signaling crosstalk between cells, prompting abnormal proliferation and aggravation of inflammatory phenotypes in various types of cells [19, 20].

Appropriate animal models are the basis of experimental research and new drug development. The AA rat model shares many similar features with RA in clinical manifestations, pathology, and immunological changes, making it a more ideal animal model to study the pathological mechanisms and evaluate drug efficacy of RA [21.22]. In addition, the AA rat model was successfully established, the characteristics of AA model were described in detail from the whole to the joint, and the evaluation indexes of the model were determined, including systemic evaluation, arthritis index, paw swelling level, movement score. In this study, the cell co-culture model and the TNF-α stimulated cell model were compared to select the suitable model for *in vitro* study. The cell co-culture model is widely used *in vitro* because of its similarity with the real internal environment [23]. FLS, as the main effector cell of RA joint synovium, contributes to and participates in synovium inflammation. VEC is not only an important part of vascular structure formation and angiogenesis, but also the material basis for the survival of FLS, which is closely related to the occurrence and development of RA [24,25]. FLS extracted from synovial tissue were used to establish a co-culture model with HUVECs to simulate synovial environment. TNF-α acts on VEC as a classical pro-inflammatory factor, which not only increase the secretion of inflammatory cytokines and angiogenic mediators (such as IL-1 and VEGF), but also damage the function of endothelial cells or lead to vascular dysfunction, resulting in vascular injury and local ischemia and hypoxia [26,27]. Therefore, TNF-α is a good stimulator acting on HUVECs to simulate inflammation and vascular injury. Our experiments have demonstrated that FLS and VEC in synovial tissue of AA rats are abnormally activated, including abnormal proliferation and angiogenesis. The comparison of *in vitro* models showed that there was no significant difference between them in the detection of experimental related indexes (including cell proliferation, secretion of angiogenic factors and PTEN expression). Finally, TNF-α was selected for the *in vitro* experiment, considering that FLS can not be guaranteed to be in the inflammatory state and the operability of the experiment in the *in vitro* co-culture experiment.

Angiogenesis, the formation of new capillaries from pre-existing vessels, is associated with inflammation and inflammatory diseases and is also a potential target for the treatment of RA. The pathogenicity of angiogenesis in RA, resulting in enhanced endothelial surface and persistent inflammatory cell infiltration, has been described to play an important role in the pathogenesis of this disease [7,28]. The angiogenesis process of RA is a programmed event. Angiogenic mediators produced by various types of cells

(including FLS, macrophages, etc) in the synovial environment activate VEC. The endothelial basement membrane and perivascular extracellular matrix are degraded by proteolytic enzymes. After that, VEC proliferate abundantly and migrate into the interstitial tissue due to the differentiation into invasive tip cells, called sprouting. The formation of capillary loops by sprouting VEC (tip cells) to synthesize new basement membranes helps to maintain the structural and functional integrity of nascent blood vessels and ultimately the formation of new capillaries [29–31]. Therefore, cell proliferation, migration and tubulogenesis *in vitro* were comprehensively studied to evaluate the vascularization ability of the cells in this study.

As more and more angiogenic mediators that activate VEC are identified, such as growth factors, proteolytic enzymes, integrins, and adhesion molecules, researchers mostly focus on this [32,33]. Previous studies by our group also focused on VEGF and found that VEGF binds to its surface receptors to activate downstream pathways of the cell and plays a role in mediating angiogenesis [15,16]. However, the discovery of novel approaches to target multiple cascades or to select upstream cascades of many pro-angiogenic factors may provide promising strategies for RA treatment, because the functions of angiogenic mediators are mostly cross regulated. As early as the 1990s, researchers found the important role of genetic factors regulating angiogenic mediators in tumor angiogenesis. For example, Bouck first reported that the inactivation of the p53 gene by mutation or deletion downregulateed the expression of thrombospondin, which induces angiogenesis [34–36]. Thus, one of the main consequences of tumor suppressor gene inactivation is to promote tumor angiogenesis, which makes people re-recognize the importance of tumor suppressor genes (and oncogenes) in the study of angiogenesis. In this study, PTEN was proved to have a negative regulatory effect on HUVEC angiogenesis in an inflammatory environment.

PI3K is an intracellular phosphatidylinositol kinase that phosphorylates PIP2 to produce PIP3 which in turn activates Akt [37]. PTEN reverses this process by removing phosphate groups. PI3K-Akt signaling plays a role in a variety of cellular functions including proliferation, survival, migration, invasion and cell metabolism [38,39]. Upstream components of the PI3K-Akt signaling pathway such as PTEN and Ras are commonly mutated in many human cancers, especially playing an important role in regulating normal vascularization and pathological angiogenesis. Direct evidence for the involvement of PI3K and Akt in regulating angiogenesis *in vivo* was observed by forced expression of PI3K and Akt by the RCAs retroviral vector system [11]. Over-expression of PI3K or Akt induces angiogenesis, whereas over-expression of PTEN inhibits angiogenesis in chicken embryos, indicating that PI3K-Akt signal is required for normal embryonic angiogenesis. In addition, PI3K is activated by growth factors and angiogenesis inducers, such as vascular endothelial growth factor (VEGF) and angiopoietins, activates Akt or other targets, and induces HIF-1 and VEGF expression to regulate angiogenesis[40,41]. PTEN deficient endothelial cells showing increased excessive angiogenesis have been demonstrated in the vasculogenesis of tumors [42,43]. Akt regulates multiple downstream targets, including nitric oxide synthase (NOS), nuclear factor kappaB (NF-κB), glycogen synthase kinase 3(GSK-3), and Jun N-terminal kinase (JNK). However, the specific target of Akt induced angiogenesis remains to be determined. Based on the comprehensive research of RA disease and PTEN signal, we proposed for the first time that PTEN-PI3K-Akt signal is

involved in the regulation mechanisms of RA angiogenesis. In the HUVECs model *in vitro*, we found that the expression levels of PTEN protein and mRNA were significantly decreased, and the expression levels of PI3K-Akt signal axis related protein and mRNA were significantly increased after TNF-α stimulation. In order to further verify the involvement of signal axis, we established a PTEN over-expression lentiviral vector. The experimental results are consistent with our expectation that the over-expression of PTEN inhibited the proliferation, migration and tubulogenesis of HUVECs *in vitro*. These findings support targeting the PTEN-PI3K-Akt signal as an effective strategy for the treatment of RA angiogenesis.

Inhibitors targeting the PI3K-Akt pathway have been developed, and these drugs can reduce VEGF secretion and angiogenesis as predicted. The traditional PI3K-Akt inhibitors LY294002 and wortmannin showed antiangiogenic activity, but these inhibitors are not suitable for human because of their toxicity and crossover inhibition of other lipid and protein kinases [44]. The treatment of traditional Chinese medicine has attracted more and more attention as an effective treatment with the emergence of new technological approaches. GE, as a iridoid glycoside obtained from *Gardenia jasminoides* Eills by modern extraction and separation technology of traditional Chinese medicine, is often used in the treatment of RA [14]. In recent years, our team has performed a lot of work around the study of the therapeutic effect and mechanism of GE on RA. Previous studies have shown that GE can restore the balance of pro/anti-angiogenic factors and inhibit VEGF-SphK1-S1P signal axis to exert anti-angiogenic effects [15]. This study supports the role of GE in up-regulating PTEN expression to inhibit synovial microvascular angiogenesis. Especially in the *in vitro* model, the cellular biological function of HUVECs was significantly inhibited. Furthermore, we found that the anti-angiogenic effect of GE may be regulated by PTEN-PI3K-Akt signal. The results obtained by lentivirus vector and specific inhibitors are consistent with our expectation that regulating PTEN-PI3K-Akt signal can significantly reduce the angiogenesis of HUVECs, which is consistent with the therapeutic effect of GE (Fig. 8).

5. Conclusion

Our current results support that the low-expression of PTEN in RA synovium is associated with excessive angiogenesis. GE effectively inhibited secondary inflammation and angiogenesis in AA rats and up-regulated the expression of PTEN. In addition, GE treatment attenuated the proliferation, migration and tubulogenesis of HUVECs, which was concerned with up-regulating PTEN and inhibiting the activation of PI3K-Akt pathway. The present findings offering a new option for therapeutic intervention of RA. Further studies are needed to determine the specific mechanism of GE up-regulating PTEN expression, and this part of the experiment is in progress.

Declarations

Funding

This work was supported by grants from the National Natural Science Foundation of China (No 81874360 and No 81073122).

Competing Interests

The authors declare that the research was conducted in the absence of any commercial or financial relationships that could be construed as a potential conflict of interest.

Author Contributions

Participated in research design: Yanghong Bu, and Prof. Wu. Conducted experiments: Yanghong Bu, Ran Deng, Yan Wang. Performed data analysis: Yanghong Bu, Ran Deng, Yan Wang. Wrote or contributed to the writing of the manuscript: Yanghong Bu.

Data Availability

The data generated in this study have been analyzed and included in this article, and unprocessed data will be available on request.

Ethics approval

All animal studies designed in this article have been approved by the experimental animal ethics committee of Anhui University of Traditional Chinese Medicine (No. ahucm-rates-2021049). It is considered that this study meets the requirements of animal ethics in animal species selection, quantity, feeding and modeling.

References

1. MacDonald IJ, Liu SC, Su CM, Wang YH, Tsai CH, Tang CH. Implications of Angiogenesis Involvement in Arthritis. *Int J Mol Sci*. 2018;19(7):2012.
2. Wang Y, Wu H, Deng R. Angiogenesis as a potential treatment strategy for rheumatoid arthritis. Eur J Pharmacol. 2021;910:174500.
3. Elshabrawy HA, Volin MV, Essani AB, et al. IL-11 facilitates a novel connection between RA joint fibroblasts and endothelial cells. Angiogenesis. 2018;21(2):215-228.
4. Balogh E, Biniecka M, Fearon U, Veale DJ, Szekanecz Z. Angiogenesis in Inflammatory Arthritis. *Isr Med Assoc J*. 2019;21(5):345-352.
5. Cimpean AM, Raica M. Historical Overview of In Vivo and In Vitro Angiogenesis Assays. *Methods Mol Biol*. 2021;2206:1-13.
6. Naito H, Iba T, Takakura N. Mechanisms of new blood-vessel formation and proliferative heterogeneity of endothelial cells. *Int Immunol*. 2020;32(5):295-305.
7. Elshabrawy HA, Chen Z, Volin MV, Ravella S, Virupannavar S, Shahrara S. The pathogenic role of angiogenesis in rheumatoid arthritis. *Angiogenesis*. 2015;18(4):433-448.
8. Xue L, Huang J, Zhang T, et al. PTEN inhibition enhances angiogenesis in an in vitro model of ischemic injury by promoting Akt phosphorylation and subsequent hypoxia inducible factor-1α

upregulation. *Metab Brain Dis*. 2018;33(5):1679-1688.

9. Liu C, He L, Wang J, et al. Anti-angiogenic effect of Shikonin in rheumatoid arthritis by downregulating PI3K/AKT and MAPKs signaling pathways. *J Ethnopharmacol*. 2020;260:113039.
10. Zhang H, Wang P, Zhang X, Zhao W, Ren H, Hu Z. SDF1/CXCR4 axis facilitates the angiogenesis via activating the PI3K/AKT pathway in degenerated discs. Mol Med Rep. 2020;22(5):4163-4172.
11. Jiang BH, Zheng JZ, Aoki M, Vogt PK. Phosphatidylinositol 3-kinase signaling mediates angiogenesis and expression of vascular endothelial growth factor in endothelial cells. Proc Natl Acad Sci U S A. 2000;97(4):1749-1753.
12. Li Q, Zhao H, Chen W, Huang P, Bi J. Human keratinocyte-derived microvesicle miRNA-21 promotes skin wound healing in diabetic rats through facilitating fibroblast function and angiogenesis. Int J Biochem Cell Biol. 2019;114:105570.
13. Lu JM, Zhang ZZ, Ma X, Fang SF, Qin XH. Repression of microRNA-21 inhibits retinal vascular endothelial cell growth and angiogenesis via PTEN dependent-PI3K/Akt/VEGF signaling pathway in diabetic retinopathy. *Exp Eye Res*. 2020;190:107886.
14. Ran D, Hong W, Yan W, Mengdie W. Properties and molecular mechanisms underlying geniposide-mediated therapeutic effects in chronic inflammatory diseases. *J Ethnopharmacol*. 2021;273:113958.
15. Wang Y, Wu H, Deng R, et al. Geniposide downregulates the VEGF/SphK1/S1P pathway and alleviates angiogenesis in rheumatoid arthritis in vivo and in vitro. Phytother Res. 2021;35(8):4347-4362.
16. Sun M, Deng R, Wang Y, et al. Sphingosine kinase 1/sphingosine 1-phosphate/sphingosine 1-phosphate receptor 1 pathway: A novel target of geniposide to inhibit angiogenesis. *Life Sci*. 2020;256:117988.
17. Cheung TT, McInnes IB. Future therapeutic targets in rheumatoid arthritis?. *Semin Immunopathol*. 2017;39(4):487-500.
18. Firestein GS, McInnes IB. Immunopathogenesis of Rheumatoid Arthritis. *Immunity*. 2017;46(2):183-196.
19. Duan MX, Zhou H, Wu QQ, et al. Andrographolide Protects against HG-Induced Inflammation, Apoptosis, Migration, and Impairment of Angiogenesis via PI3K/AKT-eNOS Signalling in HUVECs. *Mediators Inflamm*. 2019;2019:6168340.
20. Protopsaltis NJ, Liang W, Nudleman E, Ferrara N. Interleukin-22 promotes tumor angiogenesis. *Angiogenesis*. 2019;22(2):311-323.
21. Bevaart L, Vervoordeldonk MJ, Tak PP. Evaluation of therapeutic targets in animal models of arthritis: how does it relate to rheumatoid arthritis?. *Arthritis Rheum*. 2010;62(8):2192-2205.
22. Choudhary N, Bhatt LK, Prabhavalkar KS. Experimental animal models for rheumatoid arthritis. *Immunopharmacol Immunotoxicol*. 2018;40(3):193-200.

23. Noack M, Miossec P. Effects of Methotrexate Alone or Combined With Arthritis-Related Biotherapies in an *in vitro*Co-culture Model With Immune Cells and Synoviocytes. *Front Immunol*. 2019;10:2992.
24. Noack M, Miossec P. Effects of Methotrexate Alone or Combined With Arthritis-Related Biotherapies in an *in vitro*Co-culture Model With Immune Cells and Synoviocytes. *Front Immunol*. 2019;10:2992.
25. Huang TL, Mu N, Gu JT, et al. DDR2-CYR61-MMP1 Signaling Pathway Promotes Bone Erosion in Rheumatoid Arthritis Through Regulating Migration and Invasion of Fibroblast-Like Synoviocytes. *J Bone Miner Res*. 2019;34(4):779-780.
26. Ogami K, Yamaguchi R, Imoto S, et al. Computational gene network analysis reveals TNF-induced angiogenesis. BMC Syst Biol. 2012;6 Suppl 2(Suppl 2):S12.
27. Mahdavi Sharif P, Jabbari P, Razi S, Keshavarz-Fathi M, Rezaei N. Importance of TNF-alpha and its alterations in the development of cancers [published online ahead of print, 2020 Mar 21]. Cytokine. 2020;130:155066.
28. Szekanecz Z, Besenyei T, Szentpétery A, Koch AE. Angiogenesis and vasculogenesis in rheumatoid arthritis. *Curr Opin Rheumatol*. 2010;22(3):299-306.
29. Marrelli A, Cipriani P, Liakouli V, et al. Angiogenesis in rheumatoid arthritis: a disease specific process or a common response to chronic inflammation?. *Autoimmun Rev*. 2011;10(10):595-598.
30. Taylor PC, Sivakumar B. Hypoxia and angiogenesis in rheumatoid arthritis. *Curr Opin Rheumatol*. 2005;17(3):293-298.
31. Volin MV, Koch AE. Interleukin-18: a mediator of inflammation and angiogenesis in rheumatoid arthritis. *J Interferon Cytokine Res*. 2011;31(10):745-751.
32. Bosisio D, Salvi V, Gagliostro V, Sozzani S. Angiogenic and antiangiogenic chemokines. *Chem Immunol Allergy*. 2014;99:89-104.
33. Kuczynski EA, Reynolds AR. Vessel co-option and resistance to anti-angiogenic therapy. *Angiogenesis*. 2020;23(1):55-74.
34. Bouck N. P53 and angiogenesis. *Biochim Biophys Acta*. 1996;1287(1):63-66.
35. Sundaram P, Hultine S, Smith LM, et al. p53-responsive miR-194 inhibits thrombospondin-1 and promotes angiogenesis in colon cancers. *Cancer Res*. 2011;71(24):7490-7501.
36. Ren B, Yee KO, Lawler J, Khosravi-Far R. Regulation of tumor angiogenesis by thrombospondin-1. *Biochim Biophys Acta*. 2006;1765(2):178-188.
37. Chen CY, Chen J, He L, Stiles BL. PTEN: Tumor Suppressor and Metabolic Regulator. *Front Endocrinol (Lausanne)*. 2018;9:338.
38. Papa A, Pandolfi PP. The PTEN-PI3K Axis in Cancer. *Biomolecules*. 2019;9(4):153.
39. Yi J, Zhu J, Wu J, Thompson CB, Jiang X. Oncogenic activation of PI3K-AKT-mTOR signaling suppresses ferroptosis via SREBP-mediated lipogenesis. *Proc Natl Acad Sci U S A*. 2020;117(49):31189-31197.
40. Karar J, Maity A. PI3K/AKT/mTOR Pathway in Angiogenesis. *Front Mol Neurosci*. 2011;4:51.

41. Duan MX, Zhou H, Wu QQ, et al. Andrographolide Protects against HG-Induced Inflammation, Apoptosis, Migration, and Impairment of Angiogenesis via PI3K/AKT-eNOS Signalling in HUVECs. *Mediators Inflamm*. 2019;2019:6168340.
42. Serra H, Chivite I, Angulo-Urarte A, et al. PTEN mediates Notch-dependent stalk cell arrest in angiogenesis. *Nat Commun*. 2015;6:7935.
43. El Hafny-Rahbi B, Brodaczewska K, Collet G, et al. Tumour angiogenesis normalized by myo-inositol trispyrophosphate alleviates hypoxia in the microenvironment and promotes antitumor immune response. J Cell Mol Med. 2021;25(7):3284-3299.
44. Ouyang W, Li J, Shi X, Costa M, Huang C. Essential role of PI-3K, ERKs and calcium signal pathways in nickel-induced VEGF expression. Mol Cell Biochem. 2005;279(1-2):35-43.

Figures

Figure 1

Experimental flow

AA rats model was established on the left posterior paw by single subcutaneous injection of FCA (0.1 mL) at day 1. The model was evaluated from day 7 and the rats with successful modeling were orally given TG (10 mg/kg) and GE (30,60,120 mg/kg) for one week. After treatment, the serum and synovial tissue of each group were taken for *in vitro* experiment. FLS were cultured and participated in the experiment *in vitro* with HUVECs.

Figure 2

GE improved symptoms and synovial histopathological of AA rats. A. The paw observation of AA rats showed swelling (SW) and arthritic nodules (AN). B. Effects of GE on arthritis index in AA rats. C. Effects of GE on paw swelling in AA rats. D. Effects of GE on mobility score in AA rats. E. Effects of GE on the pathomorphology of synovium in AA rats. The red arrows indicate synoviocytes (S), angiogenesis (A) and inflammatory cells (I) respectively. Data are represented as mean ± SD (n = 8). $^{\#}P < 0.05$, $^{\#\#}P < 0.01$ versus control group; $^{*}P < 0.05$, $^{**}P < 0.01$ versus AA group.

Figure 3

GE inhibited angiogenesis of AA rats. A. Effects of GE on the expression of CD31, VEGF, and PTEN in synovial tissue of AA rats by immunohistochemistry (n = 6). Brownish yellow in the cytoplasm represents positive results. B. Effects of GE on the MVD in synovial tissue of AA rats was quantified by the number of CD31 positive vessels. C. Statistical analysis of average optical density of VEGF and PTEN. D. Effects of GE on VEGF level in AA rats serum (n = 4). Data are represented as mean ± SD. $^{\#}P < 0.05$, $^{\#\#}P < 0.01$ versus control group; $^{*}P < 0.05$, $^{**}P < 0.01$ versus AA group.

Figure 4

Establishment and comparison of HUVECs inflammation model *in vitro*. A. CCK-8 analysis of HUVECs proliferation treated with different concentrations of TNF-α for 24 hr (n = 6). B. CCK-8 analysis of HUVECs proliferation treated with different concentrations of FLS-CM for 24 hr (n = 6). C. Western blot analysis of PTEN protein levels treated with different concentrations of FLS-CM (n = 3). D. ELISA analysis of VEGF levels in TNF-α inflammation model and FLS-CM model (n = 6). E. Western blot analysis of PTEN protein levels in TNF-α inflammation model and FLS-CM model (n = 3). F. RT-qPCR analysis of PTEN mRNA levels in TNF-α inflammation model and FLS-CM model (n = 3). Data are represented as mean ± SD. $^{\#}P < 0.05$, $^{\#\#}P < 0.01$ versus control group.

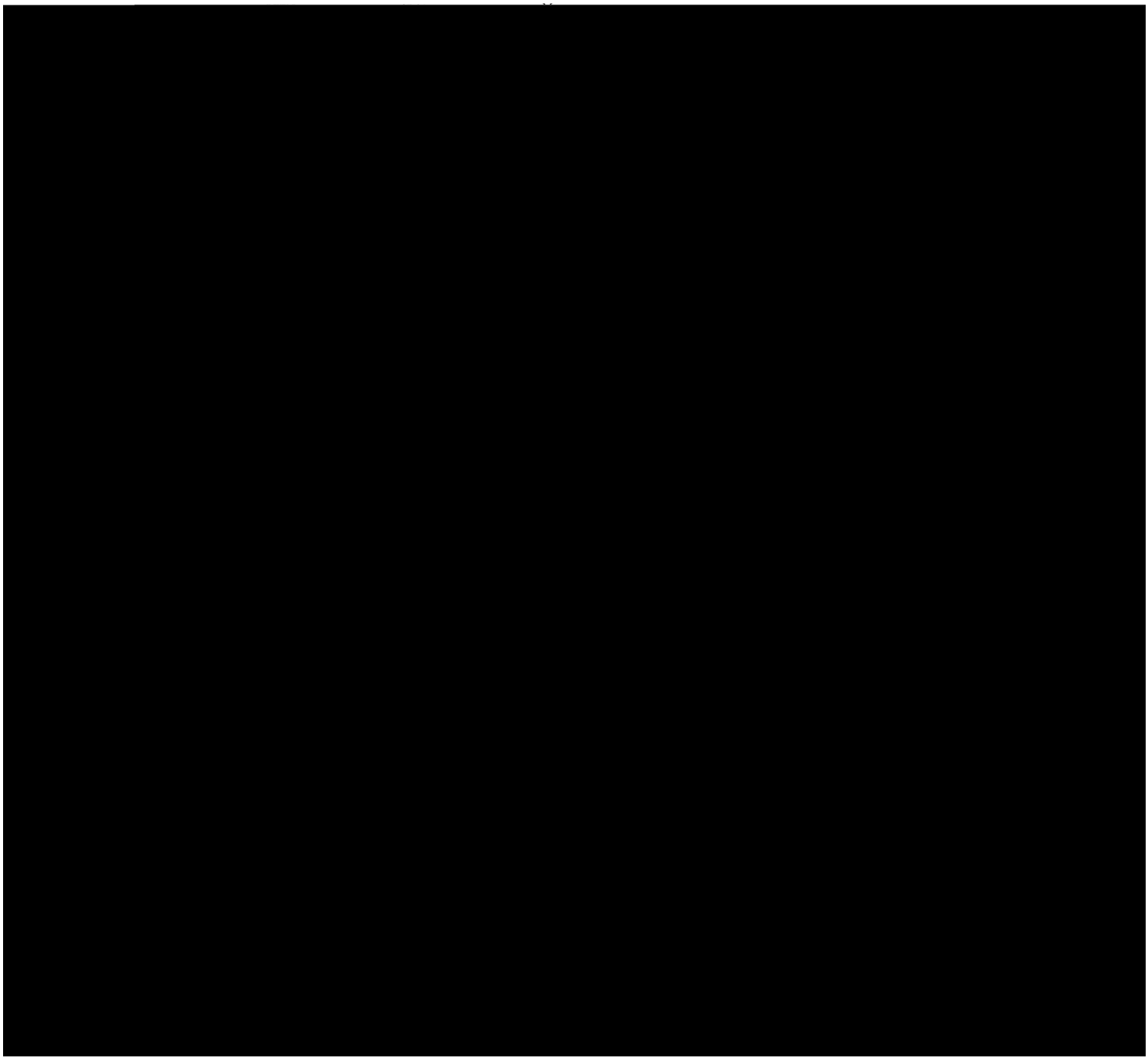

Figure 5

PTEN over-expression inhibited the proliferation, migration, and tube formation of HUVECs *in vitro*. A. The expression of PTEN by immunofluorescence after lentivirus vector infection (×200) (n = 6). B. RT-qPCR analysis of PTEN in HUVECs infected with lentivirus vector. GADPH was used as control (n = 3). C. Effects of Lv-PTEN^{+} on the cell cycle of HUVECs (n = 3). D. Effects of Lv-PTEN^{+} on the Edu expression of HUVECs (n = 6). E. Effects of Lv-PTEN^{+} on the horizontal migration of HUVECs (n = 6). F. Effects of Lv-PTEN^{+} on the vertical migration of HUVECs (n = 6). G. Effects of Lv-PTEN^{+} on the tube formation of HUVECs (n = 6). Data are represented as mean ± SD. $^{\#}P < 0.05$, $^{\#\#}P < 0.01$ versus control group.

Figure 6

GE up-regulated PTEN to inhibit angiogenesis of HUVECs *in vitro*. A. Effects of GE on the cell cycle of HUVECs (n = 3). B. Effects of GE on the Edu expression of HUVECs (n = 6). C. Effects of GE on the horizontal migration of HUVECs (n = 6). D. Effects of GE on the vertical migration of HUVECs (n = 6). E. Effects of GE on the tube formation of HUVECs (n = 6). Data are represented as mean ± SD. $^{\#}P < 0.05$, $^{\#\#}P < 0.01$ versus control group; $^{*}P < 0.05$, $^{**}P < 0.01$ versus TNF-α group.**GE up-regulated PTEN to inhibit angiogenesis of HUVECs *in vitro*.** A. Effects of GE on the cell cycle of HUVECs (n = 3). B. Effects of GE on the Edu expression of HUVECs (n = 6). C. Effects of GE on the horizontal migration of HUVECs (n = 6). D. Effects of GE on the vertical migration of HUVECs (n = 6). E. Effects of GE on the tube formation of HUVECs (n = 6). Data are represented as mean ± SD. $^{\#}P < 0.05$, $^{\#\#}P < 0.01$ versus control group; $^{*}P < 0.05$, $^{**}P < 0.01$ versus TNF-α group.

Figure 7

Effects of GE on the expression of PTEN-PI3K-Akt signaling axis in HUVECs. A. Representative Western blot band of PTEN (A), PI3K (B), p-PI3K (B), Akt (D) and p-Akt (E), and relative protein expression level. F. RT-qPCR analysis of PTEN, PI3K, and Akt in HUVECs. Data are represented as mean ± SD (n = 3). $^{\#}P < 0.05$, $^{\#\#}P < 0.01$ versus control group; $^{*}P < 0.05$, $^{**}P < 0.01$ versus TNF-α group.

Figure 8

Role of the PTEN-PI3K-Akt signaling pathway in angiogenesis of synovial tissue in RA

In the inflammatory microenvironment of synovium, PTEN expression is down-regulated to induce the activation of PI3K-Akt signaling pathway, which is involved in the changes of biological function of endothelial cells (ECs). ECs are activated and proliferate maliciously, then differentiate into tip cells and migrate to surrounding tissues and cells (synovial tissue, fibroblast-like synovial cells). In the process of migration, ECs form endothelium loop and gradually remodel into new blood vessels. Neovascularization provides nutrition and oxygen for synovial cells and tissues, and promotes the proliferation of synovial cells and tissue. Finally, the neovascularization formed by ECs and the abnormal proliferative synovial tissue interact to jointly promote the disease of RA. GE up-regulated the expression of PTEN and inhibited the activation of PI3K-Akt, so as to play an anti-angiogenesis role. This scheme shows a potential

angiogenesis mechanisms, in which the PTEN-PI3K-Akt signaling pathway may regulate the stimulation of inflammatory environment on HUVECs and the treatment of GE.